Quantitative Proteomics Reveals a Role for Epigenetic Reprogramming During Human Monocyte Differentiation

ARTICLE *in* MOLECULAR & CELLULAR PROTEOMICS · OCTOBER 2014

Impact Factor: 6.56 · DOI: 10.1074/mcp.M113.035089 · Source: PubMed

7 AUTHORS, INCLUDING:

Dequina Nicholas
Boston University
8 PUBLICATIONS **67** CITATIONS
SEE PROFILE

Jai Rudra
University of Texas Medical Branch at Galveston
25 PUBLICATIONS **670** CITATIONS
SEE PROFILE

Langridge William
Loma Linda University
153 PUBLICATIONS **1,888** CITATIONS
SEE PROFILE

Kangling Zhang
University of Texas Medical Branch at Galveston
61 PUBLICATIONS **3,551** CITATIONS
SEE PROFILE

analytical chemistry

Article

pubs.acs.org/ac

Multiplexed Parallel Reaction Monitoring Targeting Histone Modifications on the QExactive Mass Spectrometer

Hui Tang,[†] Huasheng Fang,[†] Eric Yin,[†] Allan R. Brasier,[‡] Lawrence C. Sowers,[†] and Kangling Zhang*[,†]

[†]Department of Pharmacology, University of Texas Medical Branch, Galveston, Texas 77555, United States

[‡]Institute for Translational Sciences, Sealy Center for Molecular Medicine, University of Texas Medical Branch, Galveston, Texas 77555, United States

Supporting Information

ABSTRACT: Histone acetylation and methylation play an important role in the regulation of gene expression. Irregular patterns of histone global acetylation and methylation have frequently been seen in various diseases. Quantitative analysis of these patterns is of high value for the evaluation of disease development and of outcomes from therapeutic treatment. Targeting histone acetylation and methylation by selected reaction monitoring (SRM) is one of the current quantitative methods. Here, we reported the use of the multiplexed parallel reaction monitoring (PRM) method on the QExactive mass spectrometer to target previously known lysine acetylation and methylation sites of histone H3 and H4 for the purpose of establishing precursor-product pairs for SRM. 55 modified peptides among which 29 were H3 K27/K36 modified peptides were detected from 24 targeted precursor ions included in the inclusion list. The identification was carried out directly from the trypsin digests of core histones that were separated without derivatization on a homemade capillary column packed with Waters YMC ODS-AQ reversed phase materials. Besides documenting the higher-energy c-trap dissociation (HCD) MS^2 spectra of previously known histone H3/H4 acetylated and methylated tryptic peptides, we identified novel H3 K18 methylation, H3 K27 monomethyl/acetyl duel modifications, H2B K23 acetylation, and H4 K20 acetylation in mammalian histones. The information gained from these experiments sets the foundation for quantification of histone modifications by targeted mass spectrometry methods directly from core histone samples.

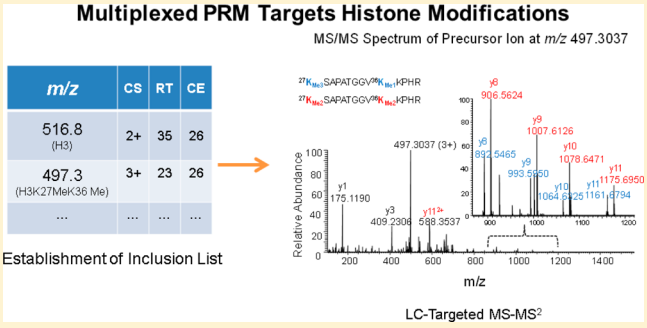

Core histones including H2A, H2B, H3, and H4 form chromatin scaffolds which are wrapped by ~147 bp DNA and bound with linker histone H 1s, transcriptional factors, and chromatin remodeling complexes to form highly ordered genome architectures, the chromosomes. These molecules in the human genome are highly modified post-translationally by acetylation, methylation, phosphorylation, ubiquitination, etc. Both histone modifications and DNA methylation comprise the epigenetic modifications that regulate gene expression. Histone acetylation is normally correlated to gene activation[1] while DNA methylation is correlated to gene repression.[2] However, regulation of gene expression by histone methylation depends on not only the sites that are methylated but also the methylation states whether they are mono-, di-, or trimethylated. For example, in many cases, H3 K4 trimethylation, K36 trimethylation, and K79 methylation activate gene expression while H3 K9 methylation, K27 methylation, and H4 K20 methylation deactivate gene expression.[3] Epigenetic modification does not remain unchanged throughout the whole lifetime of a cell; it is a dynamic process as histones are acetylated by histone acetyltransferases and deacetylated by histone deacetylases and methylated by histone methyltransferases and demethylated by histone demethylases.[4] In parallel, DNA is methylated by DNA methyltransferases (DNMT1 and DNMT 3A/B) and demethylated through oxidation (with Tet enzymes, cofactors α-ketoglutarate (αKG), and Fe^{2+}) and base excision repair (BER) pathways.[5] These dynamic modification processes are believed to play critical roles in mammalian cell development.[6]

In the past decade, mass spectrometry has made marked contribution to the epigenetic field by identification of numerous novel modifications of histones. (References were omitted because there too many to be cited and equally considered.) Many of those identified modifications have been shown to have significant biological functions. Although the identification of protein modifications including histone modifications has become less tedious compared to that of the past, owing to a significant advancement of mass spectrometers whose scan rate, resolution, and sensitivity are tremendously increased, quantification of histone modifications is still a major challenge to analytical chemistry because modifications are highly congested on histone N-termini. We

Received: March 7, 2014
Accepted: May 13, 2014
Published: May 13, 2014

   dx.doi.org/10.1021/ac500972x | *Anal. Chem.* 2014, 86, 5526−5534

thought that LC-MS-MS with selected reaction monitoring (SRM) mode on a triple quadrupole mass spectrometer (it was previously called multiple reaction monitoring (MRM) in DMPK studies in pharmaceutical industries) could be used to target histone modifications of interest and then adopted this SRM approach to quantify histone modifications in U937 leukemia cells.[7] This SRM method was also described by others for measurement of histone modification dynamics.[8] However, the success of quantification is largely dependent on correct selection of precursor ion-product ion transitions. A more complicated situation is two site modifications in one peptide such as the H3 K27/K36 peptides. Since each site can be un-, mono-, di-, and trimethylated, there are a total of 15 methylated peptides among which there are five groups of isobaric isoformers including monomethylated peptides K27me1K36me0 and K27me0K36me1; dimethylated peptides K27me2K36me0, K27me0K36me2, and K27me1K36me1; trimethylated peptides K27me3K36me0, Kme0K36me3, K27me2K36me1, and K27me1K36me2; tetra-methylated peptides K27me3K36me1, K27me2K36me2, and K27me1K36me3; and penta-methylated peptides K27me3K36 and K27me2K36me3. The situation becomes more complicated when three H3 isoforms (H3.1/3.2/3.3) and H3 S28 phosphorylation are taken into account. In order to quantify these isoformers, distinct precursor-product transitions of SRM must be found to distinguish each isoform from the other. To this end, we examined the higher-energy c-trap dissociation (HCD) fragmentation patterns and documented all the spectra associated with the targeted precursor ions of previously known H3/H4 N-terminally acetylated and methylated tryptic peptides of histone H3 and histone H4 using multiplexed parallel reaction monitoring (PRM) (Figure 1). We identified several new modifications and untangled the complex fragmentation patterns associated with H3 K27 methylation/acetylation and K36 modification peptide isoforms. This repertoire of HCD spectra provided the foundation for quantification of histone acetylation and methylation by targeted mass spectrometry approaches.

EXPERIMENTAL PROCEDURES

Cell Culture. Caco-2 cells purchased from American Type Cell Collection (ATCC) were grown in Dulbecco's Modified Eagle's Medium (DMEM) supplemented with 10% fetal bovine serum (ATCC) and 1% antibiotic-antimycotic solution (Corning) in a 75-CM^2 flask in a 37 °C, 5% CO_2 incubator.

Histone Isolation and Digestion. Collected cells (3−5 × 10^6 cells) were washed one time with phosphate buffered saline (PBS). The cell pellets were suspended in ice-cold TEB (Triton Extraction Buffer: PBS containing 0.5% triton 100, 2 mM phenylmethylsulfonyl fluoride (PMSF), 0.02 mM NaN3 and protease inhibitor cocktail (one tablet per 10 mL)) for 1 h. After centrifugation at 2000 RMP for 5 min and removal of the supernatant, the nuclei were washed once with TEB and then resuspended in 0.5 mL of 0.4 N H_2SO_4 for histone extraction. The extraction took place overnight at 4 °C. In the extraction solution, the supernatant after centrifugation at 2000 RMP for 10 min was collected and trichloroacetic acid (TCA) solution (100% (w/v)) was then added to the supernatant until there was a final concentration of ∼33% of TCA in order to precipitate core histones. After incubation for 30 min and centrifugation at 16,000 rpm for 10 min, the histone pellets were washed with −20 °C precooled acetone twice and, after removal of acetone, the histones were air-dried in a chemical hood. Dried histones were dissolved in 200 μL of D.I. water. Each time, 20 μL of histone solution was added to 50 μL of 25 mM ammonium bicarbonate solution and digested in a 37 °C incubator with a mixing speed of 60 RMP with 1.0 μg of trypsin for 10 h. The tryptic peptides were reconstituted in 0.1% formic acid and desalted by hypercarbon spin columns before subjection to mass spectrometry analysis.

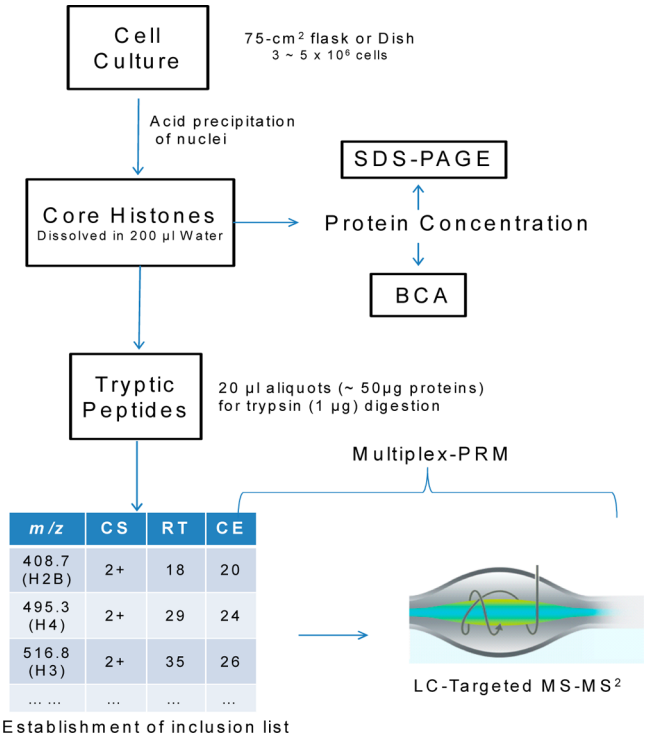

Figure 1. Flow scheme for targeting histone modifications by multiplexed parallel reaction monitoring. Core histones were isolated from cultured cells by acid precipitation, and their purities were evaluated by SDS-PAGE; concentrations were determined by BSA. An aliquot of histone solution was digested by trypsin (50:1 ratio). Histone modifications were analyzed by LC-targeted MS-MS^2 based on a preset inclusion list that includes histone inherent unmodified peptides as reference peptides.

LC-Targeted MS-MS^2 Experiments. The LC system was set as one-way mode, and the precolumn normally used in two-way mode was replaced with a second analytical column. The analytical columns (10−30 CM, 75 μM ID × 360 μM OD) were packed with packing materials scooped from a Waters YMC aqueous analytical column using a pressure bomb. Analytical separation was performed with a flow rate at 450 nL/min with a 90 min gradient of increasing CH_3CN (buffer B, 0.1% HCOOH/CH_3CN) using an Easy nano-UPLC and an autosampler. Following sample loading, buffer B was held at 2% for 5 min and slowly increased from 2% B to 15% B over 35 min, followed by a quick increase to 95% B over 10 min. After holding at 95% B for 15 min, buffer B was decreased over 5 min to 2% B and the column was re-equilibrated at 98% A for 20 min. In all experiments, HPLC eluent was introduced into the mass spectrometer via an integrated electrospray emitter operated at 2.6−2.8 kV and coupled to the Flexon nano-ESI source. QExactive experiments were performed on a quadrupole mass filter-equipped benchtop orbitrap mass spectrometer (QExactive, TFS, Bremen, Germany) with an isolation width of ±3 Th. In all experiments, a full mass spectrum at 35,000 resolution (AGC target 1 × 10^6, 100 ms maximum injection

dx.doi.org/10.1021/ac500972x | Anal. Chem. 2014, 86, 5526−5534

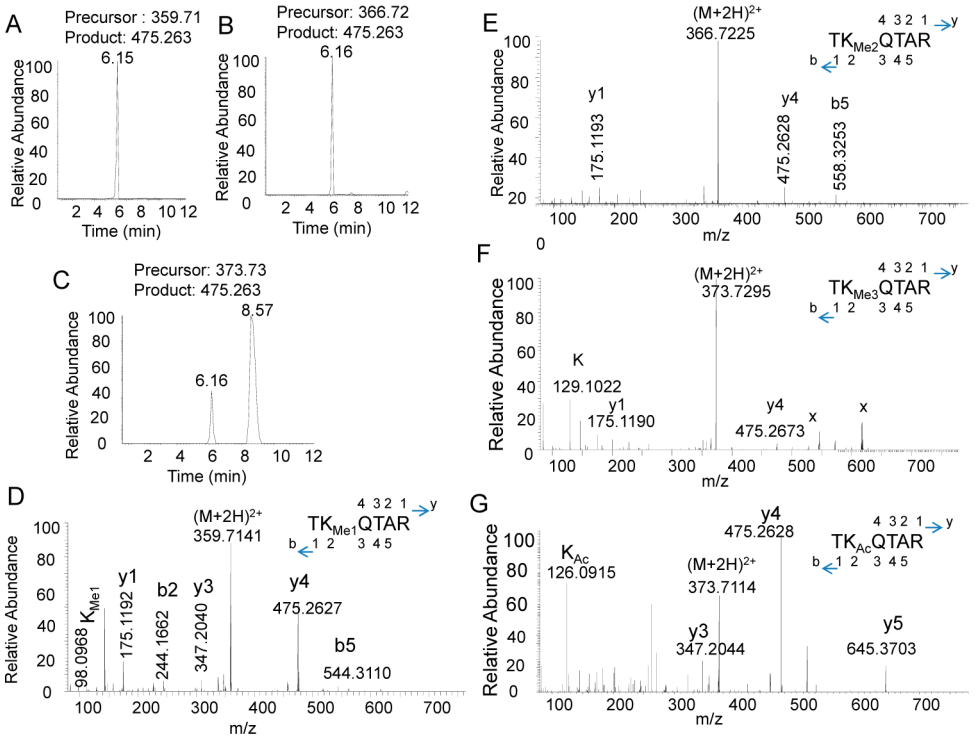

Figure 2. HCD spectra of targeted H3 K4 modified peptides. (A) TIC of product ion at m/z 475.263 dissociated from precursor ion at m/z 359.71 corresponding to H3 K4 monomethylation. (B) TIC of product ion at m/z 475.263 dissociated from precursor ion at m/z 366.72 corresponding to H3 K4 dimethylation. (C) TIC of product ion at m/z 475.263 dissociated from precursor ion at m/z 373.73 corresponding to H3 K4 trimethylation at peak 6.16 min and acetylation at 8.57 min. (D) HCD spectrum of monomethylated H3 K4 peptide. (E) HCD spectrum of dimethylated H3 K4 peptide. (F) HCD spectrum of trimethylated H3 K4 peptide. (G) HCD spectrum of acetylated H3 K4 peptide.

time, m/z 80−2000) was followed by up to 24 parallel reaction monitoring (PRM) scans at 17,500 resolution (AGC target 2×10^5, 100 ms maximum injection time) as triggered by a scheduled inclusion list (Table S1, Supporting Information). Ion activation/dissociation was performed with higher-energy c-trap dissociation (HCD).

Data Processing. Raw data has been searched against the *Homo sapiens* database with lysine acetylation and mono-, di-, and trimethylation. All spectra of modified peptides were processed by Xcalibur Qual Browser, curated by Proteome Discover 1.4 and Pinpoint 1.2, and manually confirmed with the aide of Prospector software (http://prospector.ucsf.edu/prospector/cgi-bin/msform.cgi?form=msproduct).

RESULTS

Targeted H3 K4 Methylation Identified H3 K4 Acetylation. It was not known whether H3 K4 could be acetylated until the acetylation was identified in the yeast.[9] Western-blot analysis using the antibody specific for acetylation further revealed that H3K4 in the human HeLa cell line could be acetylated as well and that HDAC3 was its specific deacetylase.[10] Mass spectrometry previously indirectly detected a trace amount of acetylation at this site in the same cell line after histone proteins were treated with propionylation.[11] Since the tryptic H3K4 peptides have only six amino acids in the sequence among which there are three hydrophilic amino acids, two threonine and one lysine, these peptides are normally washed out in the sample trap columns using conventional C18 materials resulting in no detection or entered into mass spectrometers together with solvent front or with slight retention on the column resulting in very low detection due to poor electrospray and salt suppression during the initial period of chromatography. In order to make a hydrophilic peptide retainable on the C-18 column, one option is to increase the peptide's hydrophobicity by chemical derivatization of the ε-amino group of the lysine residues in the histone proteins using alkylation reagents such as deuterated acetyl anhydride[12] or propionyl anhydride.[11] However, any remains of the alkylation reagents in the trypsin digestion buffer will alkylate the N-terminal amino groups of peptides and partially alkylate the hydroxyl groups of serine and threonine residues and monomethylated amino groups of lysine residues, which results in multiple derivatization products and thus complicated the mass spectra. Moreover, a trace amount of acetic anhydride in propionic anhydride would result in a false-positive identification of acetylation. Furthermore, propionylation is a naturally occurring modification of histones and chemical propionylation will jeopardize the identification of histone natural propionylation. In this regard, instead of changing the chemistry of peptides, we focus on making an appropriate selection of chromatographic columns that are able to retain polar peptides. On the basis of our previous experiences, YMC-pack ODS-AQ columns did a good job for separating polar compounds including histone peptides (see Experimental Procedures). In this study, we targeted H3 K4 methylation with preset doubly charged precursor ions in the inclusion list corresponding to monomethylation at m/z 359.7139, dimethylation at m/z 366.7218, and trimethylation at m/z 373.7296 9 (Table S1, Supporting Information). Methylated H3K4 peptides were eluted at 6.15−6.16 min (Figure 2A−C). As shown in Figure 2D, the HCD spectrum of m/z 359.7141 (0.2 mDa deviation from the calculated m/z) established the

dx.doi.org/10.1021/ac500972x | Anal. Chem. 2014, 86, 5526−5534

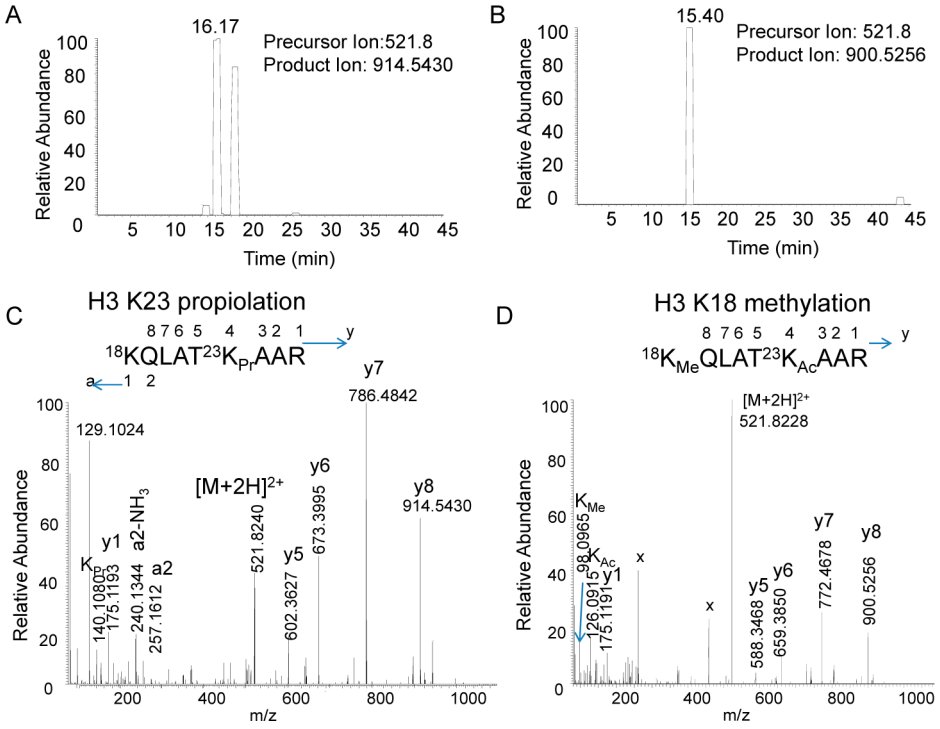

Figure 3. HCD spectra of targeted H3 K23 propionylated peptide and cotargeted H3 K18 monomethylated peptide. (A) TIC of product ion at m/z 914.5430 dissociated from the targeted precursor ion at m/z 521.8. (B) TIC of product ion at m/z 900.5256 dissociated from the targeted precursor ion at m/z 521.8. (C) HCD spectrum of H3 K23pr peptide in the 16.17 min peak as shown in (A). The peak on its right side corresponded to a nonmodified peptide. (D) HCD spectrum of H3K18meK23ac peptide. Peaks labeled "x" were from unidentified coeluted impurity.

monomethylated H3 K4 peptide sequence that was displayed on the top right of the figure. The peak at m/z 98.0968 represents the immonium ion of a monomethylated lysine. This immonium ion is a unique signature fragmentation ion of lysine monomethylation that distinguished itself from amino acid isoforms whose mass difference is also 14 Da such as glycine and analine, valine and leucine/isoleucine, and serine and theonine. Figure 2E is the HCD spectrum of m/z 366.7225 which established the dimethylated H3 K4 peptide. Trimethylation of H3 K4 was extremely low as only a weak HCD spectrum at m/z 373.7296 (0.1 mDa deviation from the calculated m/z) was detected at 6.16 min (Figure 2C) with barely observable y4 ion at m/z 475.2673 (Figure 2F). Surprisingly, the product ion (y4 at m/z 475.263) TIC of m/z 373.73 detected a second peak at 8.57 min (Figure 2C) and its intensity was higher than that of the trimethylated H3 K4 peptide peak at 6.16 min. Longer retention time indicated that this peptide was more hydrophobic than the trimethylated peptide. The measured precursor ion of the peptide at 8.57 min was m/z 373.7114 which matched the acetylated H3K4 peptide with no deviation (Figure 2G). However, it would be a 18.1 mDa or 48 ppm deviation from the trimethylated peptide. The fragmentation ion y5 at m/z 645.3703 matched an acetyl group added to K4 with only 3.9 ppm deviation from the calculated y4 at m/z 645.3678, otherwise, 52.5 ppm from trimethylated y4 at m/z 645.4042. More importantly, a significantly abundant acetylated lysine characteristic immonium ion at m/z 126.0915 was only observed in the HCD spectrum of this peptide. Furthermore, the HCD spectrum was identical to that of a tryptic acetylated H3 K4 peptide from a recombinant histone H3 (Millipore) that was previously incubated with a histone acetyltransferase (Figure S1, Supporting Information).[13] Collectively, acetylation of histone H3 K4 in human caco-2 cells was unambiguously identified and its level was significantly higher than H3 K4 trimethylation based on their peak intensities, which clearly confirmed the previous revelation of acetylation of H3 K4 in human cells by Western-blot and mass spectrometry.[9−11]

Targeted H3 K9 Methylation Identified a Total of 13 Modified Histone Peptides Including H2B K23 Acetylation. Histone H3 lysine 9 can be either acetylated or methylated. Lysine 14 is normally acetylated. Therefore, we targeted the H3 peptides with mono-, di-, and trimethylation at lysine 9 and acetylation at lysine 14 which correspond to three doubly charged precursor ions at m/z 479.2774, 486.2853, and 493.2931, respectively, to the sequences simplified as H3K9me1K14ac, H3K9me2K14ac, and H3K9me3K14ac (Table S1, Supporting Information). We did not need to specifically target the K9 acetylation peptide H3K9acK14ac with its calculated mass at m/z 493.2749 because it is very close to the mass of trimethylated K9 peptide. Targeted 479.2774-MS^2 detected H3K9me1K14ac with the sequence $^{9}K_{Me1}STGG^{14}K_{Ac}APR$ (Figure S2B, Supporting Information) and an additional six other modified histone peptides including H3.1/3.2 K27me3K36me0 with the sequence $^{27}K_{me3}SAPATGGV^{36}K$ (Figure S2C, Supporting Information), H3.1/H3.2 K27me2K36me1 with the sequence $^{27}K_{me2}SAPATGGV^{36}K_{me1}$ (Figure S2D, Supporting Information), H3.3 K27me2K36me0 with the sequence $^{27}K_{me2}SAPSTGGV^{36}K$ (Figure S2E, Supporting Information), H3.1/3.2 K27acK36me$_0$ with the sequence $^{27}K_{Ac}SAPATGGV^{36}K$ (Figure S2F, Supporting Information), H2BK16acK20ac with the sequence $^{16}K_{ac}AVT^{20}K_{ac}AQK$ (Figure S2G, Supporting Information), and H2BK20acK23ac with the sequence $AVT^{20}K_{ac}AQ^{23}K_{ac}K$ (Figure S2H, Support-

dx.doi.org/10.1021/ac500972x | Anal. Chem. 2014, 86, 5526−5534

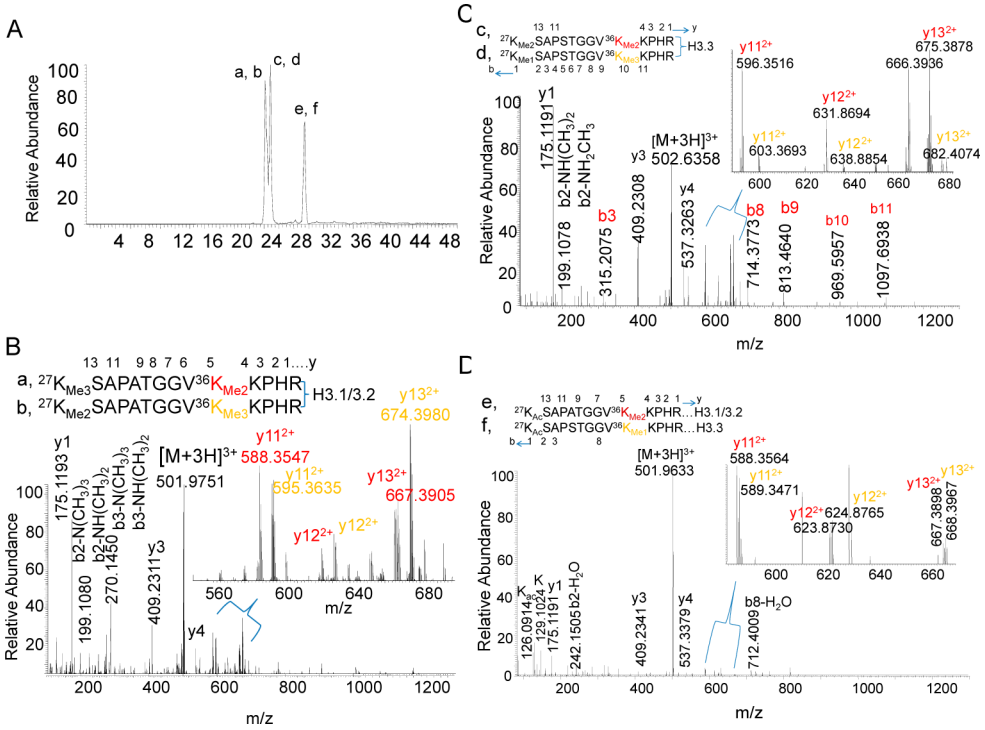

Figure 4. Targeted 501.9755-MS^2. (A) TIC of product ion at m/z 409.23 dissociated from the targeted precursor ion at m/z 501.9755. (B) HCD spectra of overlapped H3.1/3.2 K27me3K36me2 and K27me2K36me3 peptides labeled as "a, b" on the first peak shown in (A). For clarity, the neutral loss of 59.0735 ion at m/z 482.2860 (3+) and neutral loss of 45.0578 ion at m/z 486.9582, along with other fragmentation ions, were observed but not labeled. (C) HCD spectra of overlapped H3.3 K27me2K36me2 and K27me1K36me3 peptides labeled as "c, d" on the second peak shown in (A). The neutral loss of 59.0735 ion at m/z 482.9626 (3+) and neutral loss of 45.0578 ion at m/z 487.6246 were observed but not labeled. (D) HCD spectra of overlapped H3.1/3.2 K27acK36me2 and H3.3 K27acK36me1 peptides labeled as "e, f" on the third peak shown in (A).

ing Information) (Table S1, Supporting Information). Targeted m/z 486.2853-MS^2 detected H3K9me2K14ac with the sequence $^{9}K_{Me2}STGG^{14}K_{Ac}APR$ (Figure S3B, Supporting Information) and an additional two other modified histone peptides including H3.1/3.2 K27me3K36me1 with the sequence $^{27}K_{Me3}SAPATGGV^{36}K_{Me1}$ (Figure S3C, Supporting Information) and H3.3 K27acK36me0 with the sequence $^{27}K_{Ac}SAPSTGGV^{36}K$ (Figure S3D, Supporting Information). Targeted m/z 493.2931-MS^2 detected H3K9me3K14ac with the sequence $^{9}K_{Me3}STGG^{14}K_{Ac}APR$ (Figure S4B, Supporting Information) and an additional two other modified histone peptides including H3K9acK14ac with the sequence $^{9}K_{Ac}STGG^{14}K_{Ac}APR$ (Figure S4C, Supporting Information) and H2BK16acK20ac with the sequence $^{16}K_{Ac}AVT^{20}K_{Ac}VQK$ (Figure S4D, Supporting Information). H2B K5, K11, K12, K15, K16, K20, and K24 were previously identified by mass spectrometry in human small cell lung cancer carcinoma OC-NYH cells and human T lymphocyte Jurkat cells[14] as the acetylation sites. Therefore, acetylation of H2B at K23 (Figure S2H, Supporting Information) may be a novel acetylation site revealed by this study. After this site is added to the previously published sites, the N-terminal AA 1-24 of mammalian histone H2B will have a total of eight acetylation sites. Literally, all of the lysine residues in this region can be acetylated.

Targeted H3 K23 Propionylation Identifies H3 K18 Methylation. Histone H3 is normally acetylated at lysine 18 and lysine 23. It has recently been demonstrated that the lysine residues can react with longer chain CoAs such as propionyl-CoA, butyryl-CoA, and crotonyl-CoA to form propionylation, butyrylation, and crotonylation presumably using acetyltransferases as the modification enzymes.[15] We have identified hyper-propionylation of H3 K23 in undifferentiated leukemia U937 cells.[16] The chemical structure difference between propionylation and acetylation is basically only one additional methyl group. We have demonstrated that this methyl group was added to the acetyl chain to form a relatively more stable structure of propionylation instead of being added to the nitrogen of the amine group to form a relatively less stable structure of both monomethylation and acetylation at the same lysine residue. Here, we chose to target this propionylated peptide at m/z 521.84. The product ion TIC at m/z 914.5430 revealed two peaks at 16.17 and 17.50 min (Figure 3A). The HCD spectrum of precursor ion at m/z 521.8244 in the 16.17 min peak established the H3K23pr peptide with the sequence $^{18}KQLAT^{23}KprAAR$ (calculated mass of 521.8220, deviation of −3.8 ppm from the measured mass) as the N-terminal ions (b series ions) and the C-terminal fragmentation ions (y series ions) were all less than 5 ppm deviation from their theoretic masses: 175.1193 (y1, 1.7 ppm), 240.1344 (a2, 0.4 ppm), 257.1622 (b2, 1.6 ppm), 602.3628 (y5, 1.2 ppm), 673.3995 (y6, 0.6 ppm), 786.4842 (y7, 1.3 ppm), and 914.5430 (y8, 1.3 ppm) (Figure 3C). The spectrum was identical to that of an authentic H3K23pr peptide as previously reported further confirming the identification.[16] The relative intensity of this propionylated peptide to the acetylated peptide at the same site was 1/400 (or 0.25%) whose HCD spectrum was shown in Figure S5A, Supporting Information. A peak on the right side of the 16.17 min peak corresponded to a nonmodified histone peptide (spectrum not shown). Unexpectedly, targeted m/z 521.8220-MS^2 detected another peptide at retention time 15.40 min, eluted ~0.7 min ahead of the propionylated peptide. Its product ion TIC at m/z 900.5256 only displayed a single peak

dx.doi.org/10.1021/ac500972x | Anal. Chem. 2014, 86, 5526−5534

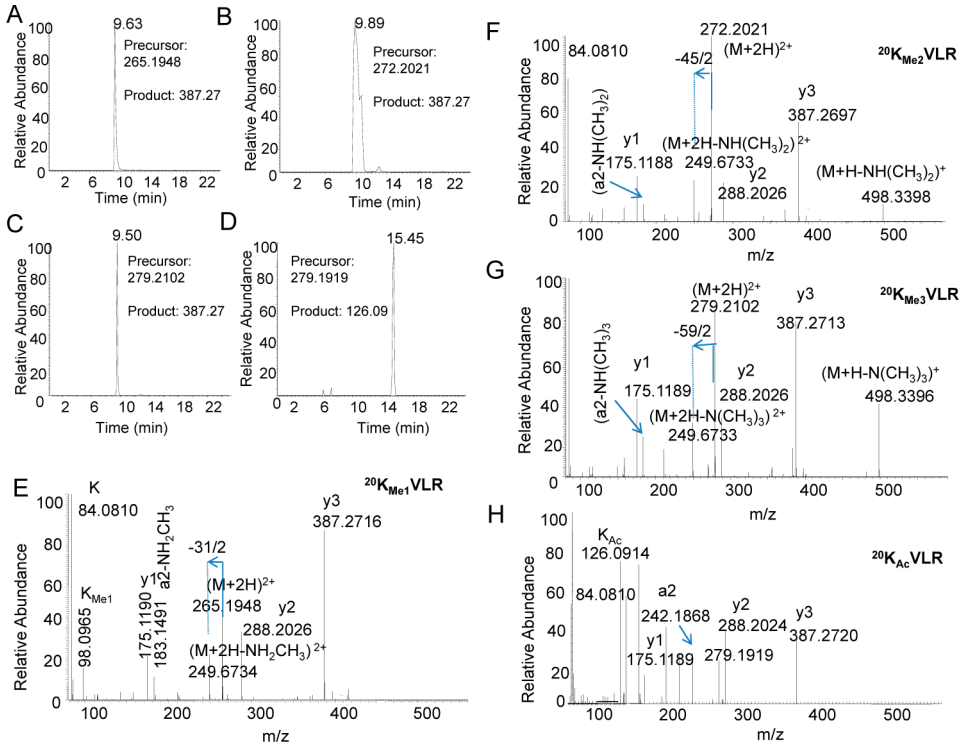

Figure 5. Targeted H4 K20 modifications. (A) TIC of product ion at m/z 387.27 dissociated from the targeted precursor ion at m/z 265.1948 corresponding to H4 K20 monomethylation. (B) TIC of product ion at m/z 387.27 dissociated from the targeted precursor ion at m/z 272.2021 corresponding to H4 K20 dimethylation. (C) TIC of product ion at m/z 387.27 dissociated from the targeted precursor ion at m/z 272.2102 corresponding to H4 K20 trimethylation. (D) TIC of product ion at m/z 126.09 dissociated from the targeted precursor ion at m/z 272.2102 corresponding to H4 K20 acetylation. (E) HCD spectrum of H4 K20 monomethylated peptide. (F) HCD spectrum of H4 K20 dimethylated peptide. (G) HCD spectrum of H4 K20 trimethylated peptide. (H) HCD spectrum of H4 K20 acetylated peptide.

at 15.40 min as shown in Figure 3B. The fragmentation ions 175.1191 (y1, 0.6 ppm), 588.3468 (y5, 0.7 ppm), 659.3850 (y6, 2.3 ppm), 772.4678 (y7, 0.3 ppm), and 900.5256 (y8, 0.6 ppm) established acetylation at K23, indicating that K18 must be methylated (Figure 3D). The observation of the monomethylated lysine signature ion at m/z 98.09649, 4.9 ppm deviation from its calculated m/z 98.09697, reinforced the assignment of monomethylation at K18. Furthermore, the identification was confirmed by an authentic peptide with the sequence $K_{Me}QLATK_{Ac}AAR$ (Figure S5C, Supporting Information). The relative intensity of K18 methylation to the same site acetylated peptide was ~1% (Figure S5B, Supporting Information).

Targeting H3 K27/K36 Methylation Identified a Total of 23 Forms of Modified K27/K36 Peptides and Revealed Complicated Isobaric Modification Patterns. The H3 K27/K36 peptides have very complicated modification states because both lysine 27 and lysine 36 can be mono-, di-, and trimethylated. Lysine 27 can also be acetylated, and its next residue serine 28 can be phosphorylated. To reduce the complexity of the present study, we set up experiments only to target K27 methylation and K36 methylation while targeting H3 K28 phosphorylation was postponed to the time when evaluation of histone phosphorylation was of specific interest. When H3 K27 trimethylation is targeted, H3 K27 acetylation is automatically targeted because there is only a 0.0102 Da difference between the triply charged acetylated precursor ions and the triply charged trimethylated precursor ions. We set up the inclusion list to target di-, tri-, tetra-, penta-, and hexa-methylation forms of K27/K36 peptides that were previously determined by LC-MS as the predominant methylation forms. The triply charged ions corresponding to these five forms of H3.1/3.2 K27/K36 methylation peptides are m/z 487.9598, 492.6317, 497.3036, 501.9755, and 506.6473. Because H3.3 K27/K36 peptides differ from H3.1/H3.2 K27/K36 peptides by only one amino acid, ^{31}A in H3.1/3.2 versus ^{31}S in H3.3, the mass difference between these two peptides is 16 Da, 2 Da (or 2/3 Da for the triply charged ion) higher than one additional methylation. Therefore, when H3.1/3.2 K27/K36 trimethylation was targeted, H3.3 K27/K36 dimethylation was targeted as well, leaving only the hexa-methylation form of H3.3 K27/K36 peptide at m/z 511.9790 (3+) to be separately targeted. Therefore, targeting the above six ions was sufficient to detect all of the 33 forms of acetylated and methylated H3 K27/K36 peptides (Table S1, Supporting Information). In order to reduce the length of the paper, targeting m/z 501.9755 ion was chosen as an example to illustrate the process of declustering the isobaric K27/K36 modification peptides using HCD product ions.

Targeted 501.9755-MS^2 detected six modified K27/K36 peptides that were eluted in three peaks labeled with "a, b", "c, d", and "e, f" according to the product ion TIC at m/z 409.23 (y3 ion) as shown in Figure 4A. Peptides a and b were determined by HCD as shown in Figure 4B as the coeluted isobaric H3.1/3.2 K27/K36 penta-methylation peptides, K27me3K36me2 and K27me2K36me3. The y ion pairs at m/z 588.3547/595.3635 ($y11^{2+}$) and 667.3905/674.3980 ($y13^{2+}$) determined K36 di- and trimethylation in these two peptides. The spectrum of these two peptide mixture is identical to the spectrum of the 1:1 mixture of two synthetic peptides,

dx.doi.org/10.1021/ac500972x | Anal. Chem. 2014, 86, 5526−5534

K27me3K36me2 and K27me2K36me3 (Figure S6, Supporting Information). Peptides c and d were determined by HCD as shown in Figure 4C as coeluted H3.3 tetra-methylation peptides, K27me2K36me2 and H3.3 K27me1K36me3. The three y ion pairs at m/z 596.3516/603.3693 ($y11^{2+}$), 631.8694/638.8854 ($y12^{2+}$), and 675.3878/682.4074 ($y13^{2+}$) determined di- and trimethylation in these two peptides. Peptides e and f that were eluted about 4 min after the previous four methylated peptides were determined by HCD as shown in Figure 4D as two acetylated peptides, H3.1/3.2 K27acK36me2 and H3.3 K27acK36me1. The appearance of m/z 126.0914 ion in the spectra of these two peptides confirmed acetylation not trimethylation at K27. Interpretation of modification identification from the HCD spectra of the other 5 targeted ions is referred to in Figures S7−S10, Supporting Information. We identified 23 out of 33 theoretical K27/K36 modification forms (Table S1, Supporting Information) from the above-mentioned six targeted ions. Including six K27/K36 peptides identified by targeting m/z 479.2774 (Figure S2C−F, Supporting Information) and 486.2853 (Figure S3C−D, Supporting Information), a total of 29 K27/K36 modification forms were identified.

Targeted H4 K20 Methylation Identifies H4 K20 Acetylation. Mammalian histone H4 is predominately dimethylated at lysine 20 with a small percent of monomethylation and trimethylation.[17] Methylation at this site together with histone H3 K9 and K27 methylation was previously reported to be associated with repressive chromatin[3] but recently revealed to be a key player in the maintenance of genomic integrity.[18] We have set up the targeted MS at m/z 265.1947, 272.2026, and 279.2103 to detect these three H4 K20 methylated peptides with sequences $^{20}K_{Me1/2/3}$VLR where lysine 20 is mono-, di-, and trimethylated. The m/z 387.27 production ion TIC of the targeted precursor ion at m/z 265.1947 showed a peak at retention time of 9.63 min (Figure 5A), and the HCD spectrum (Figure 5E) established a H4 K20 monomethylated peptide with the sequence $^{20}K_{Me1}$VLR by y1 (175.1190), y2 (288.2026), y3 (387.2716), and a2-$NH_2(CH_3)$ (183.1491) ions. The distinctive monomethylated lysine immonium ion at m/z 98.0965 was also observed, clearly demonstrating H4K20 monomethylation. Neutral loss of $NH_2(CH_3)$ ions at m/z 249.6734 (precursor-31.0422/2) and at m/z 183.1491 (a2-31.0422) further indicated a monomethylated lysine. Previously, a loss of 31 ions was typically seen in the CID mass spectrum of arginine monomethylation or symmetric dimethylation.[19] The m/z 387.27 production ion TIC of the targeted precursor ion at m/z 272.2026 showed a peak at retention time of 9.89 min (Figure 5B), and the HCD spectrum (Figure 5F) established a H4 K20 dimethylated peptide with the sequence $^{20}K_{Me2}$VLR by y1, y2, y3, and a2-$NH(CH_3)_2$ ions. Neutral loss of $NH(CH_3)_2$ ions at m/z 249.6733 (doubly charged precursor ion, 45.0578/2), 498.3398 (singly charged precursor ion, 45.0578), and 183.1491 (a2-45.0578) further indicated a dimethylated lysine. Previously, a loss of 45 ions was typically seen in the CID mass spectrum of arginine nonsymmetric dimethylation.[19] A loss of 31 and loss of 45 ions were first observed to be produced from monomethylated and dimethylated lysines, indicating that the high energy collision dissociation enhanced the formation of these neutral loss ions, and the small size of the H4 K20 peptides AA20-23 together with their neighboring hydrophobic amino acids valine and leucine might facilitate this formation. The product ion TIC at m/z 387.27 from the targeted precursor ion at m/z 279.2103 showed two peaks at retention times of 9.50 and 15.45 min (Figure 5C). The peak at 15.45 min was too low to be displayed. However, display of the product ion TIC using the acetylated lysine signature ion at m/z 126.0914 showed a distinct peak at the same location (Figure 5D), implying that the peptide in this peak might be an acetylated peptide and that its abundance was significantly lower than that of the peptide in the 9.50 min peak. The HCD spectrum at 9.50 min clearly established the H4 K20 trimethylated peptide with the sequence $^{20}K_{Me3}$VLR by y1, y2, y3, and a2-$NH(CH_3)_3$ ions (Figure 5G). Neutral loss of $N(CH_3)_3$ ions at m/z 249.6733 (doubly charged precursor ion, 59.0734/2), 498.3398 (singly charged precursor ion, 59.0734), and 183.1491 (a2-59.0735) further indicated a trimethylated lysine. However, the HCD spectrum at 15.45 min showed a distinctive fragmentation pattern from that of the trimethylated peptide (Figure 5H). The y1, y2, y3, and a2 ions at m/z 175.1189, 288.2024, 387.2720, and 242.1868 constituted the main peptide backbone K_{Ac}VLR. Determination of acetylation was based on several roles: (1) The mass accuracy of the measured precursor ion at m/z 279.1919 is a 0.2 mDa (0.7 ppm) deviation from the calculated doubly charged m/z 279.1921 of K_{Ac}VLR. However, it is 18.4 mDa (44.4 ppm) from the calculated doubly charged m/z 279.2103 of K_{Me3}VLR. (2) The a2 ion at m/z 242.1868 was only a 0.5 mDa (2.1 ppm) deviation from the calculated a2 at m/z 242.1863 corresponding to KacV while a 35.9 mDa (148.2 ppm) deviation from the calculated a2 at m/z 242.2227 corresponded to K_{Me3}V. (3) The observation of the a2 ion at m/z 242.1863 and without detection of the a2-59.0735 ion at m/z 183.1491 indicated an acetylation but not trimethylation.[20] (4) An acetylated lysine unique immonium ion at m/z 126.0914 was observed while a loss of 59.0735 ions from neither doubly charged nor singly charged precursor ions were detected. (5) An acetylated peptide has a longer retention time than a trimethylated peptide on a reversed-phase HPLC column because the former has higher hydrophobicity. Taken together, the peptide at the 15.45 min peak was unambiguously determined as the H4 K20ac peptide. We have previously identified H4K20 acetylation in *Arabidopsis*.[21] The identification of this site acetylation in human cancer cells demonstrated that H4 K20 acetylation is not plant specific. Methylation of H4K20 has been extensively studied while the function of acetylation at this site remains to be explored.

CONCLUSION

Parallel reaction monitoring (PRM) executed on the benchtop quadruple-orbitrap (QExactive) mass spectrometer has been previously demonstrated to be a potential next-generation SRM-like technology for protein targeted proteomics.[22] The PRM method performed on the orbitrap instrument was shown to have superior selectivity than a conventional SRM method that was performed on a triple-quadruple mass spectrometer because the former instrument can determine the charge states of both precursor ions and the fragmentation ions, generate highly accurate mass measurement (normally less than 5 ppm) for both precursor ions and fragmentation ions, and allow a narrow window (up to 0.2) for precursor ion selection so that the matrix and solvent background interference is significantly minimized. We set up the inclusion list including 34 precursor ions representing the currently known methylation and acetylation sites of histone H3 and H4. Targeted MS-MS^2 (HCD) of the precursor ions in this inclusion list was carried out with preset retention time and preassigned collision energy that was determined from previous runs without refinement of

dx.doi.org/10.1021/ac500972x | *Anal. Chem.* 2014, 86, 5526−5534

retention time window in a technique called multiplexed parallel selected ion monitoring-targeted proteomics as previously described.[22] While intending to apply this novel PRM method for the quantification of histone modifications, we identified several novel histone modifications.

We observed an extremely high complexity of H3 K27/K36 peptides with varying degrees of methylation statuses at K27 and K36. Just for K27 alone, it can be acetylated, methylated (mono-, di-, and trimethylation), propionylated, and modified with dual acetylation and methylation. The targeted MS-MS^2 can separate the coeluted isobaric isomers into distinguishable mono-, di-, and trimethylation at either lysine 27 or lysine 36 by declustering the overlapped HCD fragmentation ions. A distinct feature of HCD is its ability of producing abundant fingerprinting ions in the low mass region. Because the immonium ions of amino acids and modified amino acids are all located in this region (<200 Da), HCD spectra not only assist peptide sequence establishment, especially for a peptide that has amino acid F (120.0807 Da) or Y (136.0757), but also facilitate the identification of modifications.[23] Lysine residues in histones have multiple forms of modifications including acetylation and methylation which can easily be distinguished by their specific immonium ions (Figure S17, Supporting Information). Another feature of HCD is its capability of generating neutral loss ions as typically seen by loss of 31.0422 in H4 K20 monomethylated peptide, 45.0578 in H4 K20 dimethylated peptide, and 59.0735 in H4 K20 trimethylated peptide (Figure 5 and Figure S17, Supporting Information). High resolution of HCD product ions that are used to differentiate isobaric H3K27/K36 methylated peptides overcomes the poor selectivity of SRM performed on a low resolution triple quadrupole mass spectrometer. Therefore, there is no doubt that HCD in Orbitrap instruments has an unparalleled realiability for identification and quantification of histone modifications as proven through this work.

The techniques presented here also included LC-MS-MS analysis of the tryptic peptides of core histones without the need of prefractioning of core histones by HPLC and separation of histone peptides on a homemade capillary column packed with materials to retain polar compounds without the need of prederivatization of proteins with alkylation reagents. The documentation of techniques and HCD spectra of histone peptides sets the foundation for quantification of histone modifications by targeted methods including SRM on a triple quadruple mass spectrometer and PRM on a quadrupole orbitrap (or TOF) mass spectrometer. We will report such methods with stringent validation and a direct comparison between SRM and PRM for histone modifications in publications following this paper.

■ ASSOCIATED CONTENT

Supporting Information

Figures S1−S17 and Table S1. This material is available free of charge via the Internet at http://pubs.acs.org.

■ AUTHOR INFORMATION

Corresponding Author

*Tel.: 409-772-9650. E-mail: kazhang@utmb.edu.

Author Contributions

The manuscript was written through contributions of all authors. All authors have given approval to the final version of the manuscript.

Notes

The authors declare no competing financial interest.

■ ACKNOWLEDGMENTS

This work was supported by the start-up fund to K.Z. provided by Department of Pharmacology and Toxicology, School of Medicine, University of Texas Medical Branch. The authors thank Dr. Jai S. Rudra in the Department of Pharmacology, UTMB, for synthesis of histone peptides that were used for method development.

■ REFERENCES

(1) Allfrey, V. G.; Faulkner, R.; Mirsky, A. E. *Proc. Natl. Acad. Sci. U.S.A.* **1964**, *51*, 786−794.

(2) Kass, S. U.; Pruss, D.; Wolffe, A. P. *Trends Genet.* **1997**, *13* (11), 444−449.

(3) Kouzarides, T. *Cell* **2007**, *128* (4), 693−705.

(4) Zentner, G. E.; Henikoff, S. *Nat. Struct. Mol. Biol.* **2013**, *20* (3), 259−266.

(5) (a) He, Y. F.; Li, B. Z.; Li, Z.; Liu, P.; Wang, Y.; Tang, Q.; Ding, J.; Jia, Y.; Chen, Z.; Li, L.; Sun, Y.; Li, X.; Dai, Q.; Song, C. X.; Zhang, K.; He, C.; Xu, G. L. *Science* **2011**, *333* (6047), 1303−1307. (b) Ito, S.; Shen, L.; Dai, Q.; Wu, S. C.; Collins, L. B.; Swenberg, J. A.; He, C.; Zhang, Y. *Science* **2011**, *333* (6047), 1300−1303.

(6) Smith, Z. D.; Meissner, A. *Nat. Rev. Genet.* **2013**, *14* (3), 204−220.

(7) Darwanto, A.; Curtis, M. P.; Schrag, M.; Kirsch, W.; Liu, P.; Xu, G.; Neidigh, J. W.; Zhang, K. *J. Biol. Chem.* **2010**, *285* (28), 21868−21876.

(8) Zheng, Y.; Sweet, S. M.; Popovic, R.; Martinez-Garcia, E.; Tipton, J. D.; Thomas, P. M.; Licht, J. D.; Kelleher, N. L. *Proc. Natl. Acad. Sci. U.S.A.* **2012**, *109* (34), 13549−13554.

(9) (a) Maltby, V. E.; Martin, B. J.; Brind'Amour, J.; Chruscicki, A. T.; McBurney, K. L.; Schulze, J. M.; Johnson, I. J.; Hills, M.; Hentrich, T.; Kobor, M. S.; Lorincz, M. C.; Howe, L. J. *Proc. Natl. Acad. Sci. U.S.A.* **2012**, *109* (45), 18505−18510. (b) Guillemette, B.; Drogaris, P.; Lin, H. H.; Armstrong, H.; Hiragami-Hamada, K.; Imhof, A.; Bonneil, E.; Thibault, P.; Verreault, A.; Festenstein, R. J. *PLoS Genet.* **2011**, *7* (3), No. e1001354.

(10) Eot-Houllier, G.; Fulcrand, G.; Watanabe, Y.; Magnaghi-Jaulin, L.; Jaulin, C. *Genes Dev.* **2008**, *22* (19), 2639−2644.

(11) Garcia, B. A.; Hake, S. B.; Diaz, R. L.; Kauer, M.; Morris, S. A.; Recht, J.; Shabanowitz, J.; Mishra, N.; Strahl, B. D.; Allis, C. D.; Hunt, D. F. *J. Biol. Chem.* **2007**, *282* (10), 7641−7655.

(12) Smith, C. M.; Gafken, P. R.; Zhang, Z.; Gottschling, D. E.; Smith, J. B.; Smith, D. L. *Anal. Biochem.* **2003**, *316* (1), 23−33.

(13) Qian, W.; Miki, D.; Zhang, H.; Liu, Y.; Zhang, X.; Tang, K.; Kan, Y.; La, H.; Li, X.; Li, S.; Zhu, X.; Shi, X.; Zhang, K.; Pontes, O.; Chen, X.; Liu, R.; Gong, Z.; Zhu, J. K. *Science* **2012**, *336* (6087), 1445−1448.

(14) (a) Beck, H. C.; Nielsen, E. C.; Matthiesen, R.; Jensen, L. H.; Sehested, M.; Finn, P.; Grauslund, M.; Hansen, A. M.; Jensen, O. N. *Mol. Cell. Proteomics* **2006**, *5* (7), 1314−1325. (b) Bonenfant, D.; Coulot, M.; Towbin, H.; Schindler, P.; van Oostrum, J. *Mol. Cell. Proteomics* **2006**, *5* (3), 541−552.

(15) (a) Chen, Y.; Sprung, R.; Tang, Y.; Ball, H.; Sangras, B.; Kim, S. C.; Falck, J. R.; Peng, J. M.; Gu, W.; Zhao, Y. M. *Mol. Cell. Proteomics* **2007**, *6* (5), 812−819. (b) Tan, M. J.; Luo, H.; Lee, S.; Jin, F. L.; Yang, J. S.; Montellier, E.; Buchou, T.; Cheng, Z. Y.; Rousseaux, S.; Rajagopal, N.; Lu, Z. K.; Ye, Z.; Zhu, Q.; Wysocka, J.; Ye, Y.; Khochbin, S.; Ren, B.; Zhao, Y. M. *Cell* **2011**, *146* (6), 1015−1027.

(16) Liu, B.; Lin, Y.; Darwanto, A.; Song, X.; Xu, G.; Zhang, K. *J. Biol. Chem.* **2009**, *284* (47), 32288−32295.

(17) Zhang, K.; Tang, H.; Huang, L.; Blankenship, J. W.; Jones, P. R.; Xiang, F.; Yau, P. M.; Burlingame, A. L. *Anal. Biochem.* **2002**, *306* (2), 259−269.

(18) Pei, H.; Zhang, L.; Luo, K.; Qin, Y.; Chesi, M.; Fei, F.; Bergsagel, P. L.; Wang, L.; You, Z.; Lou, Z. *Nature* **2011**, *470* (7332), 124−128.

(19) (a) Brame, C. J.; Moran, M. F.; McBroom-Cerajewski, L. D. *Rapid Commun. Mass Spectrom.* **2004**, *18* (8), 877−881. (b) Zou, Y.; Wang, Y. *Biochemistry* **2005**, *44* (16), 6293−6301.
(20) Zhang, K. L.; Yau, P. M.; Chandrasekhar, B.; New, R.; Kondrat, R.; Imai, B. S.; Bradbury, M. E. *Proteomics* **2004**, *4* (1), 1−10.
(21) Zhang, K.; Sridhar, V. V.; Zhu, J.; Kapoor, A.; Zhu, J. K. *PloS One* **2007**, *2* (11), No. e1210.
(22) (a) Gallien, S.; Duriez, E.; Crone, C.; Kellmann, M.; Moehring, T.; Domon, B. *Mol. Cell. Proteomics* **2012**, *11* (12), 1709−1723. (b) Gallien, S.; Peterman, S.; Kiyonami, R.; Souady, J.; Duriez, E.; Schoen, A.; Domon, B. *Proteomics* **2012**, *12* (8), 1122−1133. (c) Peterson, A. C.; Russell, J. D.; Bailey, D. J.; Westphall, M. S.; Coon, J. J. *Mol. Cell. Proteomics* **2012**, *11* (11), 1475−1488.
(23) Olsen, J. V.; Macek, B.; Lange, O.; Makarov, A.; Horning, S.; Mann, M. *Nat. Methods* **2007**, *4* (9), 709−712.